Composites of polyvinyl alcohol (PVA) Hydrogel and calcium and magnesium phosphate formed by enzymatic functionalization

ARTICLE *in* MATERIALS LETTERS · AUGUST 2014

Impact Factor: 2.27 · DOI: 10.1016/j.matlet.2014.08.129

11 AUTHORS, INCLUDING:

Timothy E L Douglas
Ghent University
52 PUBLICATIONS **586** CITATIONS
SEE PROFILE

Lieve I L Balcaen
Ghent University
48 PUBLICATIONS **539** CITATIONS
SEE PROFILE

Ria Cornelissen
Ghent University
31 PUBLICATIONS **143** CITATIONS
SEE PROFILE

Miroslawa El Fray
West Pomeranian University of Technology…
47 PUBLICATIONS **300** CITATIONS
SEE PROFILE

Materials Letters 137 (2014) 62–67

Contents lists available at ScienceDirect

Materials Letters

journal homepage: www.elsevier.com/locate/matlet

Composites of polyvinyl alcohol (PVA) hydrogel and calcium and magnesium phosphate formed by enzymatic functionalization

Timothy E.L. Douglas [a,*], Agnieszka Piegat [b], Heidi A. Declercq [c], David Schaubroeck [d], Lieve Balcaen [e], Vitaliy Bliznuk [f], Bernhard De Meyer [g], Frank Vanhaecke [e], Ria Cornelissen [c], Miroslawa El Fray [b], Peter Dubruel [a]

[a] Polymer Chemistry and Biomaterials (PBM) Group, Department of Organic and Macromolecular Chemistry, University of Ghent, Krijgslaan 281 S4, 9000 Ghent, Belgium
[b] Division of Biomaterials and Microbiological Technologies, West Pomeranian University of Technology, Szczecin, Poland
[c] Department of Basic Medical Science—Histology Group, Ghent University, De Pintelaan 185 (6B3), 9000 Ghent, Belgium
[d] Center for Microsystems Technology (CMST), ELIS, imec, Technologiepark 914a, 9052 Ghent, Belgium
[e] Department of Analytical Chemistry, Ghent University, Krijgslaan 281 S12, 9000 Ghent, Belgium
[f] Department Material Science & Engineering, Technologiepark 903, 9052 Zwijnaarde, Belgium
[g] Polymer Chemistry Research (PCR) Group, Department of Organic Chemistry, Ghent University, Krijgslaan 281 S4, 9000 Ghent, Belgium

ARTICLE INFO

Article history:
Received 5 July 2014
Accepted 24 August 2014
Available online 4 September 2014

Keywords:
Biomaterials
Composite materials

ABSTRACT

Hydrogel biomaterials can be easily enriched with bioactive substances such as the mineralization-promoting enzyme alkaline phosphatase (ALP). In this study, poly(vinyl alcohol) (PVA) hydrogels designed for osteochondral regeneration containing incorporated ALP were mineralized with calcium phosphate (CaP) and magnesium phosphate (MgP) by incubation in solutions of 0.1 M calcium or magnesium glycerophosphate (CaGP, MgGP). Hydrogels incubated in water served as controls.

More mineral was formed in hydrogels incubated in CaGP than in MgGP. Rheometry revealed that mechanical strength (storage modulus) decreased in the order: CaGP > MgGP > water. Physicochemical characterization showed that hydrogels incubated in CaGP appeared to be mineralized with apatite and amorphous CaP, while hydrogels incubated in MgGP appeared to be mineralized with plate-like MgP crystals and amorphous MgP. Hydrogels incubated in water were devoid of mineralization. Cell viability testing showed that proliferation on hydrogels incubated in MgGP was comparable to that on non-mineralized samples and superior to that on hydrogels incubated in CaGP. The results prove the principle of enzymatic mineralization of PVA hydrogels with CaP and MgP. Further work may concentrate on in vivo evaluation of the suitability of these mineralized hydrogels for bone or osteochondral regeneration applications.

1. Introduction

Poly(vinyl alcohol) (PVA) is a widely used biocompatible synthetic polymer. Due to its solubility in water, crosslinking is necessary to form PVA hydrogel implants. Previous work has shown that repeated freeze-thaw cycles of aqueous PVA solutions result in a more crystalline, ordered structure of PVA, leading to increased interaction between PVA chains and hydrogel formation due to physical crosslinking [1]. Such hydrogels have mechanical properties similar to those of native cartilage, making them of interest as materials for cartilage repair [1,2].

In order to increase their suitability for osteochondral or bone regeneration, mineralization of such hydrogels is desirable. Advantages of the presence of a mineral phase in hydrogels include superior mechanical strength [3–5] and promotion of new bone formation [6–8]. A mineral phase can be formed in hydrogels through enzymatic action. Incorporation of the enzyme alkaline phosphatase (ALP) followed by incubation in solutions containing calcium and the enzyme substrate glycerophosphate (GP) leads to precipitation of insoluble calcium phosphate (CaP) inside the hydrogel [3,4,9–11].

By substituting Mg^{2+} ions with Ca^{2+} ions in the mineralization solution, magnesium phosphate (MgP) can be formed instead of CaP. Recently, MgP has been gaining interest as an alternative to CaP. For example, newberyite ($MgHPO_4 \cdot 3H_2O$) has demonstrated good cytocompatibility and supported osteoblast adhesion and expression of ostoblastic markers at the mRNA level [12] while

* Corresponding author. Current address: Nano & Biophotonics group, Department Molecular Biotechology, Coupure Links 653, 9000 Ghent, Belgium.
E-mail address: Timothy.Douglas@UGent.be (T.E.L. Douglas).

http://dx.doi.org/10.1016/j.matlet.2014.08.129
0167-577X/

bone cements based on struvite ($MgNH_4PO_4 \cdot 8H_2O$) have shown superior cytocompatibility to brushite and apatite [13]. Several studies have reported a stimulatory effect of magnesium as a component of CaP on bone cell proliferation [5,14–19].

In this study, enzymatic mineralization of ALP-loaded PVA hydrogels with CaP or MgP was achieved by incubation in solutions of calcium glycerophosphate (CaGP) or magnesium glycerophosphate (MgGP). The resulting mineralized hydrogels were characterized physicochemically with respect to amount and nature of mineral formed and mechanical properties. Their ability to support the growth of osteoblast-like cells was also evaluated with a view to their application as scaffolds for osteochondral and bone regeneration.

Other studies on physically crosslinked PVA hydrogels have focused on cell biological characterization with cells relevant for skin, ophthalmic or muscular tissue regeneration [20,21]. In these studies, cells adhered to and proliferated on the PVA hydrogels, demonstrating their cytocompatibility. Previous work on PVA hydrogels used in this study has focused on their physiochemical characterization in the unmineralized state [1,2]. However, this is the first study dealing with the mineralization of PVA hydrogels and their physicochemical and cell biological characterization with a cell type relevant for bone and osteochondral tissue engineering. Investigations into applications of MgP as a biomaterial usually involve pure inorganic MgP, most often in the form of struvite cements. In contrast, generation of hydrogel-inorganic composite biomaterials containing MgP remains a relatively unexplored area of research.

2. Materials and methods

Production of PVA hydrogels and ALP incorporation: Hydrogels of PVA (Elvanol 90-50, Mn=37700 g/mol, degree of hydrolysis 99–99.8%) of height 1 cm and diameter 6 mm (Fig. 1a) were prepared as described previously [1,2,22]. Briefly, a 10% (w/v) PVA solution containing 2.5 mg/ml ALP (Sigma-Aldrich, P7640) was prepared at 90 °C in the course of 12 h, poured into sample moulds and subjected to nine cycles of freezing at −18 °C for 12 h and thawing at 18 °C for 12 h.

Mineralization and rheometry: Hydrogels were incubated for 14 days in 0.1 M CaGP (Sigma-Aldrich, 50043) or 0.1 M MgGP (Sigma-Aldrich, 17766) and rinsed three times with Milli-Q water. Samples for cell biological testing were sterilized by gamma radiation generated by an Elektronika 10/10 accelerator (Institute of Nuclear Chemistry and Technology, Poland). The irradiation dose was fixed at 25 kGy. Hydrogel storage moduli (G′) were measured at 37 °C, strain 0.1%, angular frequency 10 rad/s using a Physica, MCR 301 rheometer (Anton Paar) (rotating head diameter 25 mm, sample gap 1 cm). Measurements were performed in triplicate.

Physicochemical analysis in dry state: Hydrogels where lyophilized for 48 h prior to physiochemical analysis. Dry mass percentage served as a measure of mineral formed and was calculated as: (weight after incubation and subsequent freeze-drying for 24 h/weight before freeze-drying) × 100. Thermogravimetric analysis (TGA) was performed from 25 °C to 800 °C in a nitrogen atmosphere with a heating rate of 10 °C/min using a 851e Mettler-Toledo device. Chemical and molecular structure/composition of the hydrogels was investigated using Attenuated Total Reflectance Fourier-Transform Infrared (ATR-FTIR), Scanning Transmission Electron Microscopy (STEM), Selected Area Electron Diffraction (SAED) and elemental mapping based on Energy-Dispersive X-ray Spectroscopy (EDXS) as described previously [23].

The mass and molar concentrations of elemental Ca, Mg and P and the Ca/P, Ca/Mg and Mg/P molar ratios were determined by inductively coupled plasma optical emission spectroscopy (ICP–OES) as described previously [23]. For all sample groups, $n=3$.

Scanning Electron Microscopy (SEM) was carried out on a JEOL JSM-5600 instrument in the secondary electron mode (SEI) after coating with a thin gold layer (ca 20 nm) using a plasma magnetron sputter coater as described previously [4].

Cell culture studies: Each hydrogel sample was seeded with 40,000 MG63 cells. Cell-loaded hydrogels were cultured for 14 d, after which cell viability was determined using an MTT assay as

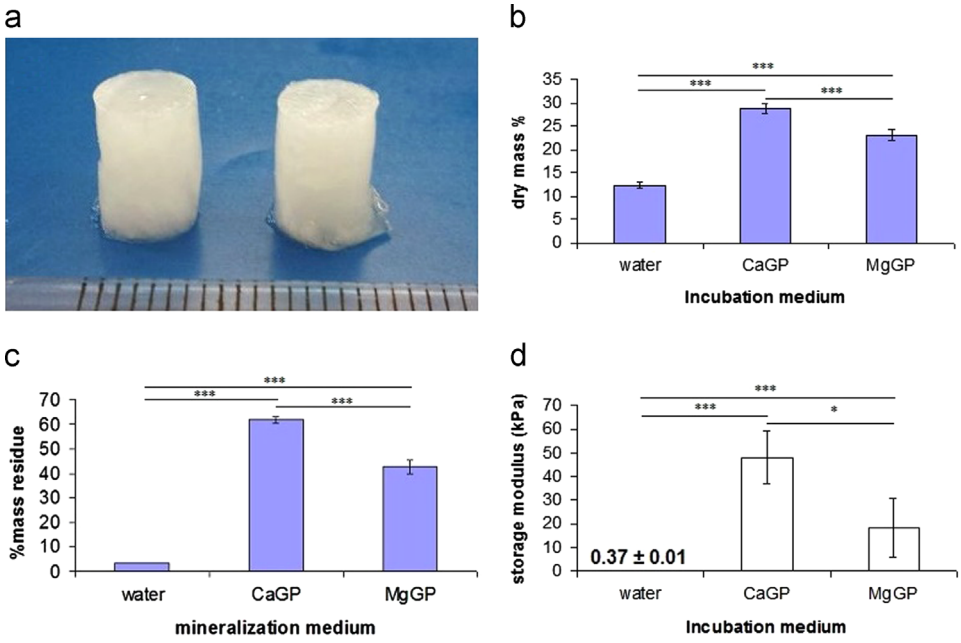

Fig. 1. (a) PVA hydrogels of height 1 cm and diameter 6 mm. (b) Dry mass percentage of PVA hydrogels incubated for 14 d in water or 0.1 M CaGP or MgGP ($n=3$). (c) TGA determination of mass percentage attributable to mineral of PVA hydrogels containing after incubation for 14 d in water or 0.1 M CaGP or MgGP ($n=3$) and lyophilization. (d) Rheometrical measurement of storage modulus of PVA hydrogels containing ALP incubated for 14 d in water, 0.1 M CaGP or 0.1 M MgGP. *$p<0.05$; ***$p<0.001$. Error bars show standard deviation.

described previously [5]. Cell viability is expressed as a percentage of the positive control (tissue culture polystyrene). For all sample groups, $n=3$.

Statsitical analysis: Significances were determined by one-way analysis of variance (ANOVA) using SPSS statistics software (IBM Corporation). The data is expressed as mean ± stand deviation (SD).

3. Results and discussion

Physiochemical characterization: Evidence of CaP and MgP formation after incubation in CaGP and MgGP, respectively, was provided by STEM EDXS-based elemental mapping (Fig. 3bii, iii, vi and vii) and ICP–OES (Table 1). Dry mass percentage decreased in the order CaGP > MgGP > water and the differences between groups were significant (Fig. 1b). The results of analysis by TGA (Fig. 1c) and ICP–OES (Table 1) were consistent with the dry mass percentages. The fact that more CaP was formed than MgP may be due to higher solubility of MgP compared to CaP. The storage moduli of hydrogels also decreased in the order CaGP > MgGP > -water (Fig. 1d). This result is consistent with the differences in mineral formed (Fig. 1b and c) but suggests that storage modulus does not increase proportionally with amount of mineral formed.

SEM analysis demonstrated that hydrogels incubated in water were devoid of mineral deposits (Fig. 2i and ii). Hydrogels incubated in CaGP displayed approximately spherical deposits of diameter 1–2 μm with rough surfaces, which were embedded in a polymer matrix (Fig. 2iii and iv). In the case of hydrogels incubated in MgGP, plate-like deposits of length up to 10 μm were observed (Fig. 2v and vi).

FTIR analyis (Fig. 3a) showed that bands characteristic for PVA became weaker in samples incubated in CaGP and MgGP. The broad band from 3100 to 3600 cm^{-1} is linked to the OH group stretching vibrations, directly connected with the inter- and intramolecular hydrogen bonds. The absorption bands in the region 2800–3000 cm^{-1} are attributed to the alkyl stretching C–H bond, at 1730 cm^{-1} and 1100 cm^{-1} to the C-O and C–O strechtching bonds of non-hydrolyzed acetate groups from PVA. Bands at 1400 cm^{-1} are attributed to C–H bending, while bands at 1380 and 1280 cm^{-1} are due to O–H bending and bands at 1100 cm^{-1} are due to C–O stretching. Samples incubated in CaGP displayed a band at approximately 1040 cm^{-1}, which is attributable to the asymmetric stretching of phosphate, as well as bands characteristic for apatite at approximately 600 cm^{-1} and 560 cm^{-1}, which are due to assymetric bending of phosphates, respectively [24]. A band at approximately 870 cm^{-1} was also seen which is attributable to HPO_4^{2-} [25], suggesting that the apatite formed is calcium-deficient. The band at approximately 600 cm^{-1} is not distict which suggests the presence of an amorphous phase. This is supported by TEM, SAED (Fig. 3bi, iv) and ICP–OES (Table 1) results. Apatite crystals have a characteristic needle-shaped morphology [26]. However, the deposits observed were irregular in shape. Diffraction rings were indistinct, suggesting low crystallinity. Furthermore, the Ca/P elemental molar ratio was 1.20 ± 0.01, which is below that for calcium-deficient apatite.

Samples incubated in MgGP showed more intense bands caracteristic of PVA than samples incubated in CaGP. This suggests that less mineral was formed in samples incubated in MgGP. Bands due to assymetric bending of phosphates were detected at approximately 600 cm^{-1} and 540 cm^{-1}. Bands at approximately 840 cm^{-1} and approximately 700 cm^{-1} were seen, which can be attributed to water vibrational modes. Three bands were seen at 1040, 990 and 950 cm^{-1} which can be attributed to assymetric stretching modes of phosphate. These bands could suggest the presence of bobierrite ($Mg_3(PO_4)_2 \cdot 8H_2O$), which is also supported by the presence of a shoulder at 3455 cm^{-1} typical for O–H stretching of crystalline water [27]. The plate-like deposits seen by SEM (Fig. 2v, vi) may possibly also be indicative of bobierrite [12,28]. Evidence of the presence of an amorphous phase is provided by the indistinct SAED pattern (Fig. 2b, viii) and Mg/P elemental molar ratio of 1.33 ± 0.01 determined by ICP–OES (Table 1), which is lower than that of bobierrite.

Table 1
ICP–OES determination of elemental Ca, P and Mg mass percentages, elemental molar concentrations of Ca, P and Mg per unit mass sample (mmol/mg) and elemental molar ratios Ca/Mg, Ca/P and Mg/P in PVA hydrogels containing incubated for 14 d in water or 0.1 M CaGP or MgGP with subsequent lyophilization. Values are presented as mean ± standard deviation (s.d.) ($n=3$). b.d.l.: below detection limit of apparatus, hence uncalculable.

Medium	Incubation time (d)	Mass percentage element in samples					
		Ca		**P**		**Mg**	
		%	s.d.	%	s.d.	%	s.d.
Water	14	b.d.l.	b.d.l.	b.d.l.	b.d.l.	b.d.l.	b.d.l.
CaGP	14	19.2	0.3	12.3	0.3	b.d.l.	b.d.l.
MgGP	14	b.d.l.	b.d.l.	9.5	0.2	9.7	0.2
Medium	Incubation time (d)	mmol element/mg sample					
		Ca		**P**		**Mg**	
		mmol/mg	s.d.	mmol/mg	s.d.	mmol/mg	s.d.
Water	14	b.d.l.	b.d.l.	b.d.l.	b.d.l.	b.d.l.	b.d.l.
CaGP	14	4.8	0.1	4.0	0.1	b.d.l.	b.d.l.
MgGP	14	b.d.l.	b.d.l.	4.0	0.1	3.0	0.1
Medium	Incubation time (d)	Molar elemental ratios					
		Ca/Mg		**Ca/P**		**Mg/P**	
		mmol/mg	s.d.	mmol/mg	s.d.	mmol/mg	s.d.
Water	14	b.d.l.	b.d.l.	b.d.l.	b.d.l.	b.d.l.	b.d.l.
CaGP	14	b.d.l.	b.d.l.	1.20	0.01	b.d.l.	b.d.l.
MgGP	14	b.d.l.	b.d.l.	b.d.l.	b.d.l.	1.33	0.01

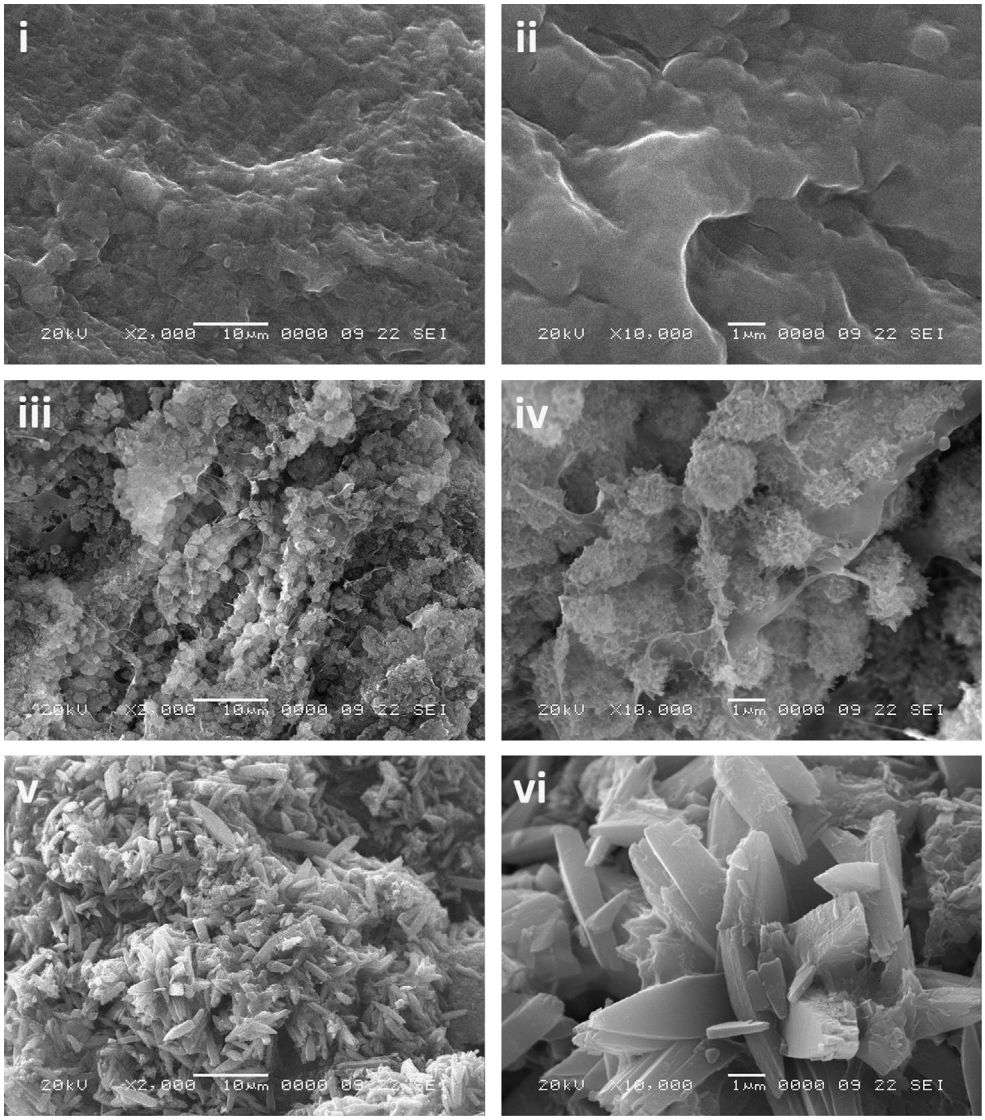

Fig. 2. SEM images of PVA hydrogels containing ALP incubated for 14 d in water (i) and (ii), 0.1 M CaGP (iii) and (iv) or 0.1 M MgGP (v) and (vi) with subsequent lyophilization. Scale bar = 10 µm (i), (iii), (v) or 1 µm (ii), (iv), (vi).

Cell biological characterization: MG63 cell growth on hydrogels incubated in water, CaGP and MgGP was markedly lower than on controls (Fig. 4). Cell viability was significantly lower on hydrogels incubated in CaGP compared to those incubated in water. Viability on hydrogels incubated in MgGP was higher than on those incubated in CaGP, but not significantly. No significant difference was observed between hydrogels incubated in water and MgGP.

The results in the present study suggest that PVA hydrogels are able to support only a limited cell attachment and/or growth of MG63 cells. PVA hydrogels are known to be intrinsically cell nonadhesive, as confirmed by the results of Gupta et al., who discovered inferior adhesion and growth of fibroblasts and myoblasts on 10% PVA (w/v) hydrogels after 4 h, 24 h and 3 d compared to glass controls [20,21]. In the present study cell growth was not promoted by mineralization, in contrast to previous studies involving enzymatic mineralization of the cell nonadhesive hydrogel gellan gum with CaP and MgP [3,5]. The reasons for these differences, as well as the lower proliferation on hydrogels mineralized with CaP, remain unclear. It is not inconceivable that calcium was released from hydrogels mineralized with CaP, especially as an amorphous phase was present (Fig. 3a, bi, iv and Table 1). This might possibly have resulted in calcium concentrations toxic for osteoblasts and a decrease in cell number, as reported by other authors [29]. One explanation for the higher viability on hydrogels mineralized with MgP compared to those mineralized with CaP may be a stimulatory influence of magnesium on cell adhesion and/or proliferation, as described by other authors [5,14–19].

4. Conclusions and outlook

CaP and MgP mineral formation in PVA hydrogels containing ALP was induced by incubation in solutions of CaGP and MgGP. More CaP was formed than MgP and hydrogels mineralized with CaP formed were mechanically stronger. CaP formed appeared to be a mixture of calcium-deficient apatite and amorphous CaP. MgP formed also appeared to be partly crystalline and partly amorphous.

Further material characterization is necessary to determine differences in surface stiffness, surface roughness and surface chemistry, which are known to influence cell adhesion,

proliferation, and differentiation [30–33]. Surface roughness values of hydrogel contact lenses have been measured using Atomic Force Microscopy (AFM) [34–36], which however have a much higher polymer content (38–67% (w/v)) than the hydrogels used in this study (10% (w/v)). Development of AFM-based techniques to determine surface roughness of mineralized and unmineralized hydrogels would be a useful analytical tool and remains a topic for further study.

Further work may also concentrate on improvement of cell growth in vitro and in vivo evaluation of the suitability of these mineralized hydrogels for bone or osteochondral regeneration applications.

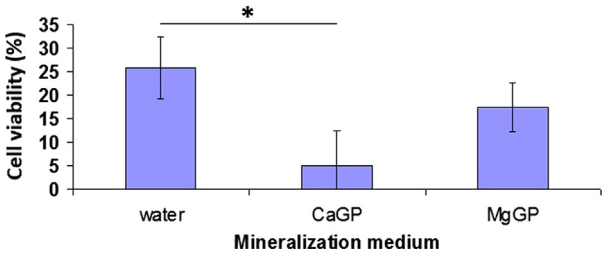

Fig. 4. Cell viability of MG63 osteoblast-like cells cultured on hydrogel samples for 14 days. Viability is expressed as a percentage of the control. Error bars show standard deviation. $^{*}p = 0.028 < 0.05$.

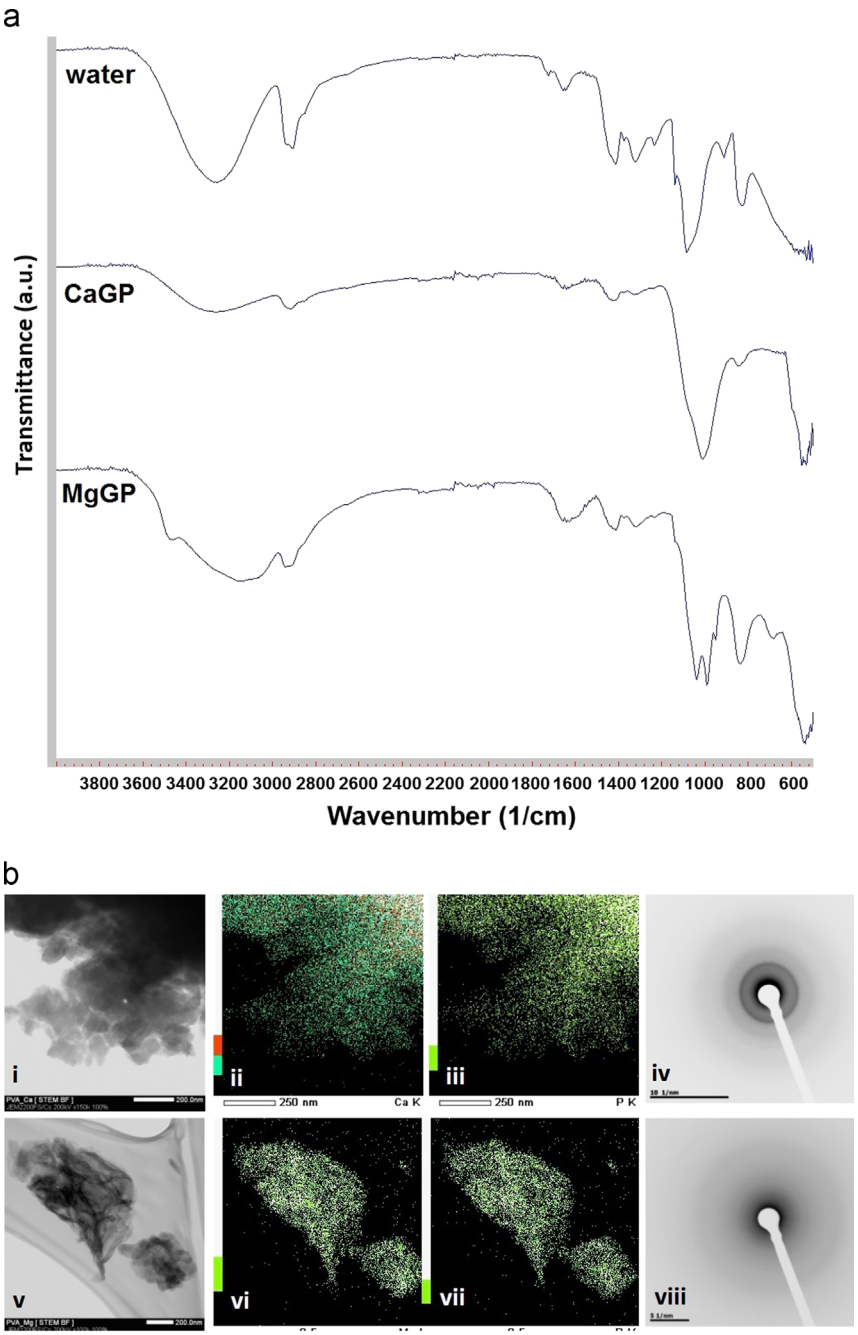

Fig. 3. (a) FTIR spectra of PVA hydrogels containing ALP incubated for 14 d in water, 0.1 M CaGP or 0.1 M MgGP. (b) STEM images of mineral formed in hydrogels after incubation in CaGP (i) and MgGP (v), EDXS-based elemental mapping of calcium (ii), magnesium (vi) and phosphorous (iii) and (vii) and SAED diffraction patterns after incubation in CaGP (iv) and MgGP (viii).

Acknowledgement and conflict of interest statement

T.E.L.D. acknowledges FWO, Belgium for a postdoctoral fellowship. H.A.D. acknowledges Ghent University for a BOF-postdoc grant. The authors have no conflict of interest.

References

[1] Pilaszkiewicz A, et al. Chemically and physically crosslinked poly(vinyl alcohol) hydrogels for cartilage repair. E-Polymers 2005;P013:1–6.
[2] El Fray M, et al. Morphology assessment of chemically modified and cryostructured poly(vinyl alcohol) hydrogel. Eur Polym J 2007;43(5):2035–40.
[3] Douglas T, et al. Enzymatic mineralization of gellan gum hydrogel for bone tissue-engineering applications and its enhancement by polydopamine. J Tissue Eng Regen Med 2012.
[4] Douglas TE, et al. Enzymatic mineralization of hydrogels for bone tissue engineering by incorporation of alkaline phosphatase. Macromol Biosci 2012;12(8):1077–89.
[5] Douglas TEL, et al. Generation of composites for bone tissue engineering applications consisting of gellan gum hydrogels mineralized with calcium and magnesium phosphate phases by enzymatic means. J Tissue Eng Regen Med 2014.
[6] Anderson JM, et al. Biphasic peptide amphiphile nanomatrix embedded with hydroxyapatite nanoparticles for stimulated osteoinductive response. ACS Nano 2011;5(12):9463–79.
[7] Hulsart-Billstrom G, et al. Calcium phosphates compounds in conjunction with hydrogel as carrier for BMP-2: a study on ectopic bone formation in rats. Acta Biomater 2011;7(8):3042–9.
[8] Suzawa Y, et al. Regenerative behavior of biomineral/agarose composite gels as bone grafting materials in rat cranial defects. J Biomed Mater Res Part A 2010;93(3):965–75.
[9] Douglas TE, et al. Enzymatically induced mineralization of platelet-rich fibrin. J Biomed Mater Res Part A 2012;100(5):1335–46.
[10] Douglas TE, et al. Acceleration of gelation and promotion of mineralization of chitosan hydrogels by alkaline phosphatase. Int J Biol Macromol 2013;56C:122–32.
[11] Filmon R, et al. Poly(2-hydroxy ethyl methacrylate)-alkaline phosphatase: a composite biomaterial allowing in vitro studies of bisphosphonates on the mineralization process. J Biomater Sci Polym Ed 2000;11(8):849–68.
[12] Tamimi F, et al. Biocompatibility of magnesium phosphate minerals and their stability under physiological conditions. Acta Biomater 2011;7(6):2678–85.
[13] Ewald A, et al. Effect of cold-setting calcium- and magnesium phosphate matrices on protein expression in osteoblastic cells. J Biomed Mater Res Part B 2011;96(2):326–32.
[14] Boanini E, et al. Magnesium and strontium doped octacalcium phosphate thin films by matrix assisted pulsed laser evaporation. J Inorg Biochem 2012;107(1):65–72.
[15] Bracci B, et al. Effect of Mg(2+), Sr(2+), and Mn(2+) on the chemico-physical and in vitro biological properties of calcium phosphate biomimetic coatings. J Inorg Biochem 2009;103(12):1666–74.
[16] Cai YL, et al. Osteoblastic cell response on fluoridated hydroxyapatite coatings: the effect of magnesium incorporation. Biomed Mater 2010;5(5):054114.
[17] Sader MS, Legeros RZ, Soares GA. Human osteoblasts adhesion and proliferation on magnesium-substituted tricalcium phosphate dense tablets. J Mater Sci Mater Med 2009;20(2):521–7.
[18] Xue W, et al. Synthesis and characterization of tricalcium phosphate with Zn and Mg based dopants. J Mater Sci Mater Med 2008;19(7):2669–77.
[19] Landi E, et al. Biomimetic Mg-substituted hydroxyapatite: from synthesis to in vivo behaviour. J Mater Sci Mater Med 2008;19(1):239–47.
[20] Gupta S, et al. Stiffness- and wettability-dependent myoblast cell compatibility of transparent poly(vinyl alcohol) hydrogels. J Biomed Mater Res Part B 2012;101(2):346–54.
[21] Gupta S, Webster TJ, Sinha A. Evolution of PVA gels prepared without crosslinking agents as a cell adhesive surface. J Mater Sci Mater Med 2011;22(7):1763–72.
[22] Peppas NA, Tennenhouse D. Semicrystalline poly(vinyl alcohol) films and their blends with poly(acrylic acid) and poly(ethylene glycol) for drug delivery applications. J Drug Delivery Sci Technol 2004;14(4):291–7.
[23] Gassling V, et al. Magnesium-enhanced enzymatically mineralized platelet-rich fibrin for bone regeneration applications. Biomed Mater 2013;8(5):055001.
[24] Pleshko N, Boskey A, Mendelsohn R. Novel infrared spectroscopic method for the determination of crystallinity of hydroxyapatite minerals. Biophys J 1991;60(4):786–93.
[25] Koutsopoulos S. Synthesis and characterization of hydroxyapatite crystals: a review study on the analytical methods. J Biomed Mater Res 2002;62:600–12.
[26] Juhasz JA, Best SM, Bonfield W. Preparation of novel bioactive nano-calcium phosphate–hydrogel composites. Sci Technol Adv Mater 2010:11.
[27] Frost RL, et al. Raman and infrared spectroscopic study of the vivianite-group phosphates vivianite, baricite, and bobierrite. Mineral Mag 2002;66:1063–73.
[28] Rivadeneyra A, et al. Precipitation of phosphate minerals by microorganisms isolated from a fixed-biofilm reactor used for the treatment of domestic wastewater. Int J Environ Res Public Health 2014;11(4):3689–704.
[29] Maeno S, et al. The effect of calcium ion concentration on osteoblast viability, proliferation and differentiation in monolayer and 3D culture. Biomaterials 2005;26(23):4847–55.
[30] Evans ND, et al. Substrate stiffness affects early differentiation events in embryonic stem cells. Eur Cell Mater 2009;18:1–13 (discussion 13-4).
[31] Rowlands AS, George PA, Cooper-White JJ. Directing osteogenic and myogenic differentiation of MSCs: interplay of stiffness and adhesive ligand presentation. Am J Physiol Cell Physiol 2008;295(4):C1037–44.
[32] Boyan BD, et al. Osteoblasts generate an osteogenic microenvironment when grown on surfaces with rough microtopographies. Eur Cell Mater 2003;6:22–7.
[33] Durand B, Gao FB, Raff M. Accumulation of the cyclin-dependent kinase inhibitor p27/Kip1 and the timing of oligodendrocyte differentiation. EMBO J 1997;16(2):306–17.
[34] Torrent-Burgues J, Sanz F. AFM in mode Peak Force applied to the study of unworn contact lenses. Colloids Surf, B 2014.
[35] Bettuelli M, et al. Surface properties and wear performances of siloxane-hydrogel contact lenses. J Biomed Mater Res Part B 2013;101(8):1585–93.
[36] Giraldez MJ, et al. Contact lens hydrophobicity and roughness effects on bacterial adhesion. Optom Vis Sci 2010;87(6):E426–31.